

Continuity of Ce 4*f* electronic structure across the quantum critical point: A resonant photoemission study on CeNi_{1-x}Co_xGe₂

H. J. Im,^{1,*} Takahiro Ito,^{1,2} J. B. Hong,³ Shin-ichi Kimura,^{1,2} and Y. S. Kwon³

¹*School of Physical Sciences, The Graduate University for Advanced Studies, Okazaki 444-8585, Japan*

²*UVSOR Facility, Institute for Molecular Science, Okazaki 444-8585, Japan*

³*BK21 Physics Research Division and Institute of Basic Science, Sungkyunkwan University, Suwon 440-746, Korea*

(Received 7 September 2005; published 20 December 2005)

Ce 3*d*-4*f* and 4*d*-4*f* resonant photoemission spectroscopies have been performed on the heavy-fermion compound CeNi_{1-x}Co_xGe₂, where the ground-state properties systematically change from the magnetic ($0 \leq x < 0.3$) to nonmagnetic ($0.3 < x \leq 1.0$) regime via the quantum critical point (QCP, $x=0.3$). Co-substitution dependence of the bulk Ce 4*f* electronic structure shows gradual evolution of Kondo resonance at the Fermi level together with the reduction of the Ce 4*f*⁰ final state in agreement with the single impurity Anderson model (SIAM). The SIAM analysis shows that the Kondo temperature and specific-heat coefficient change continuously from the weakly hybridized CeNiGe₂ to strongly hybridized CeCoGe₂. These indicate that the Ce 4*f* electronic structure of CeNi_{1-x}Co_xGe₂ changes continuously through the QCP.

DOI: [10.1103/PhysRevB.72.220405](https://doi.org/10.1103/PhysRevB.72.220405)

PACS number(s): 75.20.Hr, 71.27.+a, 79.60.-i

Heavy-fermion Ce intermetallic compounds have attracted much attention due to their wide variety of anomalous physical properties, including the non-Fermi liquid (NFL) behavior at the quantum critical point (QCP) and the heavy-fermion superconductivity.^{1,2} The scaling of these anomalous properties has been described by the Doniach phase diagram,³ where the competing energy scales of Kondo effect (T_K) and RKKY interaction (T_{RKKY}) categorize the Ce 4*f* properties from the magnetic ($T_K < T_{RKKY}$) to nonmagnetic ($T_K > T_{RKKY}$) regime through QCP ($T_K \sim T_{RKKY}$). As the system changes from the magnetic regime to QCP, the energy scale of the magnetic ordering, the Néel temperature (T_N), increases showing similar behavior to T_{RKKY} for $T_K \ll T_{RKKY}$, then is suppressed and finally disappears at the QCP due to the competition between T_K and T_{RKKY} (Ref. 1). Interestingly, the discontinuity of the Fermi surface volume through the QCP has been reported on the heavy-fermion compound YbRh₂Si₂ (Ref. 4), having been attributed to the quasi-two-dimensional spatially “localized” spin fluctuations^{5,6} as in CeCu_{5.9}Au_{0.1} (Ref. 7). On the contrary, the no discontinuity has been expected from the spin-density-wave (SDW) formation caused by the “itinerant” spin fluctuations.^{8,9} Thus the understanding of the Ce 4*f* electronic structure through a QCP is essential to elucidate the anomalous ground-state properties of strongly correlated electron systems.

It is well known that a photoemission (PE) spectroscopy is one of the most powerful methods to directly observe the density of states as well as the quasiparticle band structure. Recent progress of the experimental technique makes it possible to determine the essential bulk electronic structure¹⁰ as well as low-energy excitation such as quantum critical properties.¹¹ To clarify the character of Ce 4*f* electrons causing the various anomalous properties, many PE experiments have been performed on the Ce 4*f* heavy-fermion system.¹²⁻¹⁸ It has been believed that the Ce 4*f* electronic structure should be understood in the single impurity Anderson model (SIAM), treating the hybridization between the localized Ce 4*f* spin and conduction *spd* electrons as an or-

der parameter to form the Kondo singlet.^{5,13,19} Indeed, the Ce 4*f* electronic structure as well as the Kondo temperature have been reproduced well at both the weak¹⁵⁻¹⁷ and strong hybridization regimes,^{12-14,18} whose ground states are the magnetism and nonmagnetism, respectively. However, there are few reports concentrating on the (continuous or discontinuous) variation of the electronic structure across QCP except for the scaling with T_K among the different compounds with different crystal structures.^{10,12,13} To extract the intrinsic properties, the extrinsic effect such as the different crystal structure must be eliminated. Therefore the isostructural Ce compounds (CeNi_{1-x}Co_xGe₂) measured here are suitable for the investigation of the intrinsic change of the electronic structure across QCP.

CeNi_{1-x}Co_xGe₂ has been recently reported as one of the heavy-fermion electron systems, where the ground-state properties of Ce 4*f* electrons are tuned by the Co concentration (x) (Ref. 20). While CeNiGe₂ shows the two-step antiferromagnetic ordering ($T_N=4$ and 3 K) (Ref. 21), CeCoGe₂ is categorized as a nonmagnetic heavy-fermion system.²² With increasing Co-concentration, CeNi_{1-x}Co_xGe₂ system shifts from the magnetic ($0 \leq x < 0.3$) to nonmagnetic ($0.3 < x \leq 1$) regime through QCP ($x=0.3$), where the typical NFL behavior ($T_N \sim 0$ K, $\rho \propto T$, $\gamma \propto -\ln T$) has been observed. It should be noted that the jump of the Kondo temperature from $T_K=21$ ($x=0.6$) to 110 K ($x=0.7$) estimated by the specific heat (SH) measurements is ascribed to the additional transition of the crystal electric-field (CEF) splitting (or degeneracy of Ce 4*f* ground states; N_f). An important point is that there has been observed little change of the lattice constants at the same orthorhombic CeNiSi₂-type (*Cmcm*) crystal structure as a function of Co concentration. This strongly implies that the tuning of the anomalous properties in CeNi_{1-x}Co_xGe₂ is only caused by the change of hybridization between Ce 4*f* and Ni/Co 3*d* electrons. Hence, we can evaluate the intrinsic change of the ground-state properties through QCP only with the change of the hybridization intensity.

In this communication, we report the systematic studies of

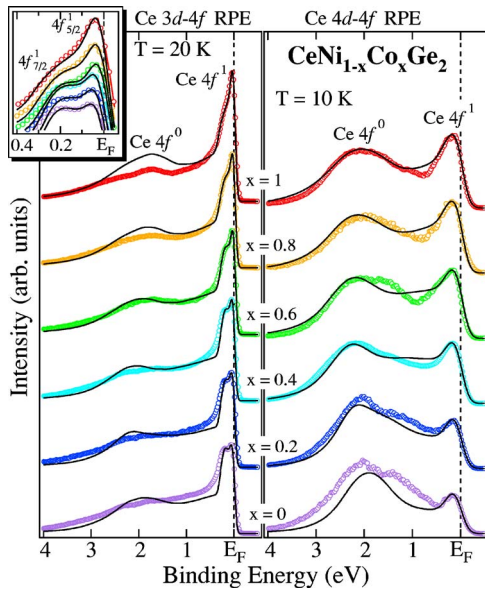


FIG. 1. (Color online) Ce 4f spectra of the experiments (circles) and its fitting results of the NCA calculation (Ref. 23) (lines) in Ce 3d-4f (left) and Ce 4d-4f (right) RPE for $\text{CeNi}_{1-x}\text{Co}_x\text{Ge}_2$. The inset shows the same ones in Ce 3d-4f RPE with enlarged scale.

the heavy-fermion compounds $\text{CeNi}_{1-x}\text{Co}_x\text{Ge}_2$ ($0 \leq x \leq 1$) by using the combination of Ce 3d-4f and 4d-4f resonant photoemission (RPE) spectroscopies to extract the essential change of the “bulk” Ce 4f electronic structure. Ce 4f spectra and the quantitative analysis based on SIAM in the non-crossing approximation (NCA) reveal that the Ce 4f electronic structure continuously changes from the weak hybridization to strong hybridization regime through QCP.

Polycrystalline samples of $\text{CeNi}_{1-x}\text{Co}_x\text{Ge}_2$ ($0 \leq x \leq 1$) were prepared by the arc melting under argon atmosphere and annealed at 900 °C for three weeks in evacuated quartz tubes. Metallographic analysis ensures that the samples used in this study are in single phase. Ce 3d-4f RPE measurements had been performed at BL25SU of SPring-8, whereas Ce 4d-4f RPE measurements were performed at BL5U of UVSOR-II, Institute for Molecular Science. The total energy resolutions and the acquired temperatures were about $\Delta E \sim 100$ meV, $T=20$ K for the Ce 3d-4f RPE, and $\Delta E \sim 300$ meV, $T=10$ K for the Ce 4d-4f RPE. The clean surfaces were prepared by *in situ* fracturing the polycrystalline samples under a vacuum of 2×10^{-8} Pa. The Fermi level (E_F) of the sample was referred to a gold film.

Figure 1 shows the Co-substitution (x) dependence of Ce 4f spectra (circles). Each Ce 4f spectrum is obtained by subtracting photon-flux-normalized off-RPE [$h\nu = 874.4$ (115) eV] spectrum from on-RPE [$h\nu = 881.3$ (122) eV] spectrum across Ce 3d(4d)-4f absorption edge at the same fractured surface. Backgrounds are removed by the nominal Shirley correction,²⁴ and the Ce 4f spectra are normalized to the same area. Two typical Ce 4f structures at around 2 eV and at $E_F - 0.3$ eV binding energies are observed. The former is ascribed to the Ce $4f^0$ final state with localized (poorly screened) Ce 4f character, while the latter to the Ce $4f^1$ final state forming the tails of the Kondo resonance (Ce $4f_{5/2}^1$) at E_F with itinerant (well-screened)

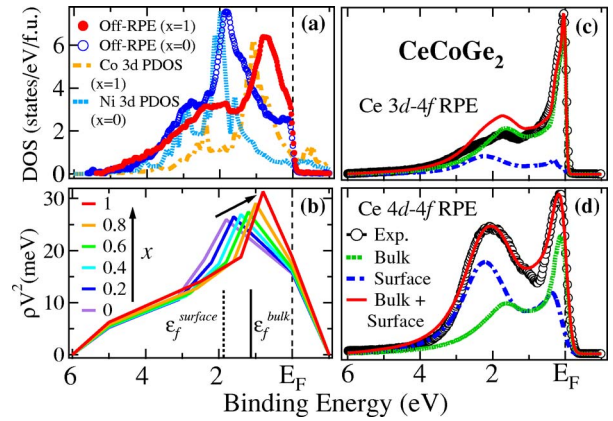


FIG. 2. (Color online) (a) The off-RPE spectra and the 3d PDOS (Co and Ni) for $x=0, 1$, obtained from Ce 3d-4f RPE and the corresponding LDA band calculation, (Ref. 25), respectively. (b) Hybridization matrix elements of bulk contribution used for the NCA calculation. (Ref. 23). Ce 4f spectra of CeCoGe_2 and the NCA fitting curves, Gaussian convoluted with the instrumental energy resolution, for (c) Ce 3d-4f RPE and (d) Ce 4d-4f RPE.

character, following the spin-orbit splitting sideband (Ce $4f_{7/2}^1$). With increasing x , the intensity ratio of Ce $4f^1$ to Ce $4f^0$ peak increases as shown in Fig. 1, which indicates the increase of the hybridization strength between the Ce 4f and Ni/Co 3d orbitals. The similar tendency also appears just below E_F where the relative intensity of the Ce $4f_{5/2}^1$ compared with the Ce $4f_{7/2}^1$ gradually increases from CeNiGe_2 to CeCoGe_2 (see inset of Fig. 1).

Figure 2(a) shows the Ce 3d-4f off-RPE spectra ($h\nu = 874.4$ eV) of CeNiGe_2 and CeCoGe_2 in comparison with the Ni/Co 3d partial density of states (PDOS) of each compound computed by the local-density approximation (LDA) band calculation using WIEN2K code.²⁵ In the figure, we find that the off-RPE spectrum of CeNiGe_2 (CeCoGe_2) is formed by an intense peak at 1.8 (0.8) eV with broad shoulders at around 2–4 eV and at $E_F - 1$ eV. The observed good correspondences between experiment and calculation indicate that the Ni/Co 3d state is dominant in the off-RPE spectra. With increasing Co concentration, the off-RPE spectra show gradual change of the energy position of the intense 3d peak, while the broad shoulders are almost unchanged (not shown). This strongly suggests that the Co-substitution dependence of the cf hybridization strength $\rho V^2(E)$ is dominated by the Ni/Co 3d electrons in $\text{CeNi}_{1-x}\text{Co}_x\text{Ge}_2$. In order to address the role of the cf hybridization in $\text{CeNi}_{1-x}\text{Co}_x\text{Ge}_2$, namely, to understand the nature of Ce 4f electrons in its electronic (magnetic) properties, the fitting by SIAM using the NCA method²³ was performed.

Figures 2(c) and 2(d) show the results of NCA calculation (solid lines) of CeCoGe_2 , where the result on the bulk (dashed lines) and surface (dot-dashed lines) components are summed up with considering the difference of surface sensitivities between the Ce 4f spectra derived by the Ce 3d-4f [Fig. 2(c)] and Ce 4d-4f [Fig. 2(d)] RPE spectrum. Here, the surface sensitivity (surface/bulk intensity ratio I_s/I_b) is given by $\exp[d/(\lambda \cos \theta)] - 1$, where d and λ are the thickness of the surface layer (\sim the nearest-neighbor Ce-Ce distance) and the mean-free path of photoelectrons as a function of

kinetic energy, respectively.²⁶ As a result, the surface sensitivity as ~ 0.28 and ~ 1.4 for Ce 3*d*-4*f* ($\lambda \sim 17$ Å) and Ce 4*d*-4*f* ($\lambda \sim 4.7$ Å) RPE spectra, respectively, was evaluated.^{10,17} The experimental spectra can be fitted by SIAM as shown in Figs. 2(c) and 2(d). To analyze the Co-substitution dependence of the Ce 4*f* spectra, we have used the identical parameters for each compound other than the shape of hybridization matrix elements $\rho V^2(E)$ as shown in Fig. 2(b).

In Fig. 2(b), the Co-substitution dependence of $\rho V^2(E)$ of bulk contribution reflects the gradual change of Ce 3*d*-4*f* off-RPE spectra from CeNiGe₂ ($x=0$) to CeCoGe₂ ($x=1$), especially considering both the energy shift of intense 3*d* peak positions from 1.8 to 0.8 eV binding energies and the change of the hybridization strength. The surface component of $\rho V^2(E)$ is modeled on the bulk derived one multiplied by 0.4–0.99 to get the best fitting between experiment and calculation. Consequently, the $\rho V^2(E_F)$ increases as a function of Co concentration in rough agreement with the itinerant nature of CeCoGe₂. For the calculation, the identical parameters used here are as follows: $\varepsilon_f^{\text{bulk(surface)}} = 1.1$ (1.9) eV, $\Delta_{SO} = 320$ meV, and $T_{3d(4d)} = 20$ (10) K, where $\varepsilon_f^{\text{bulk(surface)}}$ is the bare Ce 4*f* level for the bulk (surface) contribution, Δ_{SO} is the excitation energy from Ce 4*f*_{5/2}¹ to 4*f*_{7/2}¹ states, and $T_{3d(4d)}$ is the measurement temperature for Ce 3*d*(4*d*)-4*f* RPE. For the energy positions of the CEF splitting level $\Delta_{CEF1(CEF2)}$ and the degeneracy of the Ce 4*f* state N_f , we used the values interpolated from the SH estimations.^{20,31}

The results of the calculation of CeNi_{1-x}Co_xGe₂ are superimposed in Fig. 1 (solid lines), comparing with the experimental Ce 4*f* spectra (circles). The calculation results well reproduce both the bulk-sensitive Ce 3*d*-4*f* and surface-sensitive Ce 4*d*-4*f* RPE spectra in Fig. 1, which indicates the validity of the selected fitting parameters [$\rho V^2(E)$]. Furthermore, the quantitative consistency of T_K between the present RPE and thermodynamic experiments as shown in Fig. 3(b) is another evidence of the appropriate analysis in Fig. 2. These all suggest that we can extract the “intrinsic” change of the hybridization strength at the bulk causing the various ground states of the compounds from the magnetic to non-magnetic regime via the QCP.

Figure 3 shows the Co-substitution dependence of $\rho V^2(E_F)$, n_f , T_K , and γ obtained by the spectral fitting as shown in Fig. 1 (solid circles), being compared with T_K and γ in the thermodynamic experiments (open circles).²² Here, $\rho V^2(E_F)$ is the bulk hybridization strength at E_F , n_f the Ce 4*f* electron number obtained by the present analysis, T_K the Kondo temperature following the relation $k_B T_K = N_f \rho V^2(E_F) \times [(1-n_f)/n_f]$,¹² and γ the SH coefficient following the relation $\gamma = N_A \pi k_B (N_f - 1) / 6 T_0$, where N_A is the Avogadro's number, and T_0 the characteristic temperature ($T_0 = 1.29 T_K$ for $N_f = 2$ and $T_0 \approx T_K$ for others).²⁷ In Fig. 3(a), $\rho V^2(E_F)$ gradually increases with the Co substitution as is already discussed, while n_f gradually decreases. This reveals that the Ce 4*f* electron character continuously changes from CeNiGe₂ to CeCoGe₂. When we compare T_K and γ from PE spectra with the thermodynamic experiment,²² we find an excellent consistency [Figs. 3(b) and 3(c)] other than the

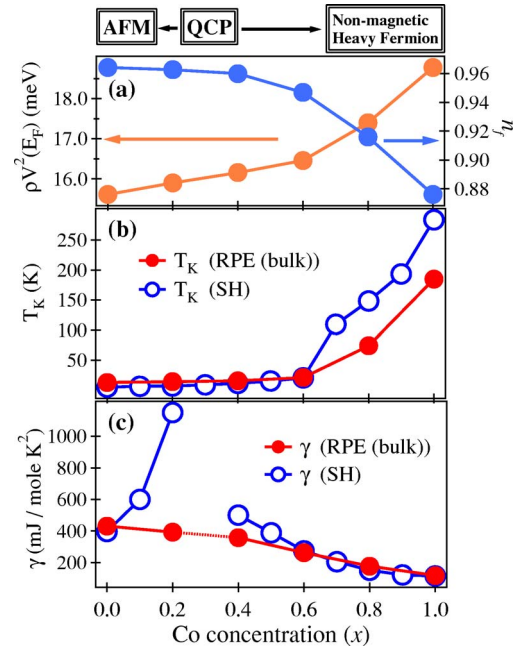


FIG. 3. (Color online) (a) Hybridization matrix intensity at E_F and Ce 4*f* electron number evaluated from NCA calculation (Ref. 23) for the bulk contribution. (b) The Kondo temperature, T_K , and (c) the specific heat coefficient, γ , obtained from PE and the SH measurement. (Ref. 20).

divergence around $x=0.3$ (QCP) of γ estimated from the SH measurement. The characteristic divergence of γ due to the logarithmic temperature dependence of C/T at QCP has been ascribed to the characteristic feature of the NFL phenomena.²² The origin has been attributed to two different scenarios. One is the spin fluctuation in the “localized” point of view and the other the SDW in the “itinerant.” Both of them indicate that the origin is the competition between the antiferromagnetism and the Kondo effect. Photoemission spectra as well as the SIAM analysis cannot include the magnetic characters but only detect the charge. Therefore, the observed enhancement on γ values evaluated by SH in contrast to the RPE measurement at around QCP indicates the magnetic contribution. This result is consistent with the spin fluctuation nature remaining below T_K at QCP. (Refs. 28 and 29).

Finally, we briefly comment on the nature of the fluctuation from the continuous change of the Ce 4*f* electronic structures through QCP. The continuity of the Ce 4*f* electronic structure seems to imply the “itinerant” character of the spin fluctuation as in 3*d* strongly correlated electron systems. But the good applicability of SIAM through QCP to understand the Ce 4*f* electronic properties near E_F is favorable to the “localized” nature of the spin fluctuation. The recent fashion of the QCP theory on the 4*f* electron systems also suggests the spatially “localized” character of the spin fluctuation,^{5,6} where the discontinuity of the Fermi surface at QCP is expected as observed in the Hall-effect measurement on YbRh₂Si₂ (Ref. 4). There are, however, no reports that suggest the anomalous change of the Fermi surface through the QCP on CeNi_{1-x}Co_xGe₂. Therefore we speculate the possible origin of the discontinuity of the Fermi surface through

the QCP, if exists, the conduction *spd* dominating band at E_F other than the Ce $4f$ dominating one. To elucidate further details of the evolution of the electronic structure through QCP, higher-resolution PE measurements at lower temperatures comparable to the magnetic ordering temperature, as well as compatible studies on other Ce $4f$ electron systems such as CeNiGe_{2-x}Si_x (Ref. 30), CeCu_{6-x}Au_x (Ref. 7), etc., are needed.

We wish to acknowledge the support of Professor O. Sakai, Professor K. Mimura, and Dr. A. Chainani for the

NCA calculation program and the fruitful discussion. This work was performed with the joint studies program of the Institute for Molecular Science (2004) and with the approval of the Japan Synchrotron Radiation Research Institute (Proposal No. 2004A0196-NSa-np), and was partially supported by the Korea Science and Engineering Foundation through the Center for Strongly Correlated Materials Research (CSCMR) at Seoul National University, and by Grant No. R01-2003-000-10095-0 from the Basic Research Program of the Korea Science and Engineering Foundation.

*Electronic address: hojun@ims.ac.jp

- ¹G. R. Stewart, *Rev. Mod. Phys.* **73**, 797 (2001).
- ²N. D. Mathur, F. M. Grosche, S. R. Julian, I. R. Walker, D. M. Freye, R. K. W. Haselwimmer, and G. G. Lonzarich, *Nature (London)* **394**, 39 (1998).
- ³S. Doniach, *Physica B & C* **91B**, 231 (1977).
- ⁴S. Paschen, T. Luhmann, S. Werth, P. Gegenwart, O. Trovarelli, C. Geibel, F. Steglich, P. Coleman, and Q. Si, *Nature (London)* **432**, 881 (2004).
- ⁵P. Coleman, *Nature (London)* **413**, 788 (2001).
- ⁶Q. Si, S. Rabello, K. Ingersent, and J. L. Smith, *Nature (London)* **413**, 804 (2001).
- ⁷A. Schroder, G. Aeppli, R. Coldea, M. Adams, O. Stockert, H. v. Lohneysen, E. Bucher, R. Ramazashvili, and P. Coleman, *Nature (London)* **407**, 351 (2000).
- ⁸J. A. Hertz, *Phys. Rev. B* **14**, 1165 (1976).
- ⁹A. J. Millis, *Phys. Rev. B* **48**, 7183 (1993).
- ¹⁰A. Sekiyama, T. Iwasaki, K. Matsuda, Y. Saitoh, Y. Onuki, and S. Suga, *Nature (London)* **403**, 396 (2000).
- ¹¹T. Valla, A. V. Fedorov, P. D. Johnson, B. O. Wells, S. L. Hulbert, Q. Li, G. D. Gu, and N. Koshizuka, *Science* **285**, 2110 (1999).
- ¹²D. Malterre, M. Grioni, and Y. Baer, *Adv. Phys.* **45**, 299 (1996).
- ¹³J. W. Allen, S. J. Oh, O. Gunnarsson, K. Schonhammer, M. B. Maple, M. S. Torikachvili, and I. Lindau, *Adv. Phys.* **35**, 275 (1986).
- ¹⁴F. Reinert, D. Ehm, S. Schmidt, G. Nicolay, S. Hufner, J. Kroha, O. Trovarelli, and C. Geibel, *Phys. Rev. Lett.* **87**, 106401 (2001).
- ¹⁵H.-D. Kim, O. Tjernberg, G. Chiaia, H. Kumigashira, T. Takahashi, L. Duo, O. Sakai, M. Kasaya, and I. Lindau, *Phys. Rev. B* **56**, 1620 (1997).
- ¹⁶H. Kumigashira, A. Chainani, T. Yokoya, O. Akaki, T. Takahashi, M. Ito, M. Kasaya, and O. Sakai, *Phys. Rev. B* **53**, 2565 (1996).
- ¹⁷T. Iwasaki, A. Sekiyama, A. Yamasaki, M. Okazaki, K. Kadono, H. Utsunomiya, S. Imada, Y. Saitoh, T. Muro, T. Matsushita *et al.*, *Phys. Rev. B* **65**, 195109 (2002).
- ¹⁸R.-J. Jung, B.-H. Choi, S.-J. Oh, H.-D. Kim, E.-J. Cho, T. Iwasaki, A. Sekiyama, S. Imada, S. Suga, and J.-G. Park, *Phys. Rev. Lett.* **91**, 157601 (2003).
- ¹⁹O. Gunnarsson and K. Schonhammer, *Phys. Rev. B* **28**, 4315 (1983).
- ²⁰B. K. Lee, J. B. Hong, J. W. Kim, K.-H. Jang, E. D. Mun, M. H. Jung, S. Kimura, T. Park, J.-G. Park, and Y. S. Kwon, *Phys. Rev. B* **71**, 214433 (2005).
- ²¹M. H. Jung, N. Harrison, A. H. Lacerda, H. Nakotte, P. G. Pagliuso, J. L. Sarrao, and J. D. Thompson, *Phys. Rev. B* **66**, 054420 (2002).
- ²²E. D. Mun, B. K. Lee, Y. S. Kwon, and M. H. Jung, *Phys. Rev. B* **69**, 085113 (2004).
- ²³O. Sakai, M. Motizuki, and T. Kasuya, *Core-Level Spectroscopy in Condensed Systems* (Springer-Verlag, Berlin/Heidelberg, 1988).
- ²⁴D. A. Shirley, *Phys. Rev. B* **5**, 4709 (1972).
- ²⁵P. Blaha, K. Schwarz, G. Madsen, D. Kvasnicka, and J. Luitz, *WIEN2K, An Augmented Plane Wave+Local Orbitals Program for Calculating Crystal Properties* (Karlheinz Schwarz Technical University Wien, Austria, 2001).
- ²⁶S. Tanuma, C. J. Powell, and D. R. Penn, *Surf. Sci.* **192**, L847 (1987).
- ²⁷F. Patthey, J.-M. Imer, W.-D. Schneider, H. Beck, Y. Baer, and B. Delley, *Phys. Rev. B* **42**, 8864 (1990).
- ²⁸J. Sichelschmidt, V. A. Ivanshin, J. Ferstl, C. Geibel, and F. Steglich, *Phys. Rev. Lett.* **91**, 156401 (2003).
- ²⁹K. Ishida, K. Okamoto, Y. Kawasaki, Y. Kitaoka, O. Trovarelli, C. Geibel, and F. Steglich, *Phys. Rev. Lett.* **89**, 107202 (2002).
- ³⁰D. Y. Kim, D. H. Ryu, J. B. Hong, J.-G. Park, Y. S. Kwon, M. A. Jung, M. H. Jung, N. Takeda, M. Ishikawa, and S. Kimura, *J. Phys.: Condens. Matter* **16**, 8323 (2004).
- ³¹The SH estimations of Δ_{CEF1} and Δ_{CEF2} were based on the Coqblin-Schrieffer model where $j=1/2$ ($N_f=2$) for $0 \leq x \leq 0.6$, $j=3/2$ ($N_f=4$) for $0.6 < x \leq 0.8$, and $j=5/2$ ($N_f=6$) for $0.9 \leq x \leq 1.0$ were expected. By interpolating the SH values, we obtained the following parameters: Δ_{CEF1} and Δ_{CEF2} ; 13 and 46 meV for $x=0$ and 0.2; 10 and 38 meV for $x=0.4$; 4 and 18 meV for $x=0.6$; 6 meV for $x=0.8$. Note that the crystal-field splitting being consistent with the SH value has been observed on high-resolution PE spectrum on CeNiGe₂ [H.J. Im *et al.*, *Physica B* (to be published)].